# Control of interfaces on electrical properties of SiO2–Parylene-C laminar composite dielectrics

**ARTICLE** *in* JOURNAL OF COLLOID AND INTERFACE SCIENCE · APRIL 2009

Impact Factor: 3.37 · DOI: 10.1016/j.jcis.2008.12.060 · Source: PubMed



**4 AUTHORS**, INCLUDING:

Ramakrishnan Rajagopalan
Pennsylvania State University
**85** PUBLICATIONS **770** CITATIONS
SEE PROFILE

Eugene Furman
Pennsylvania State University
**81** PUBLICATIONS **1,516** CITATIONS
SEE PROFILE

M. T. Lanagan
Pennsylvania State University
**269** PUBLICATIONS **2,259** CITATIONS
SEE PROFILE

Journal of Colloid and Interface Science 332 (2009) 65–73

Contents lists available at ScienceDirect

Journal of Colloid and Interface Science

www.elsevier.com/locate/jcis

# Control of interfaces on electrical properties of $SiO_2$–Parylene-C laminar composite dielectrics

Pratyush Tewari *, Ramakrishnan Rajagopalan, Eugene Furman, Michael T. Lanagan

*Materials Research Institute, The Pennsylvania State University, University Park, PA 16802, USA*

ARTICLE INFO

*Article history:*
Received 6 July 2008
Accepted 21 December 2008
Available online 25 December 2008

*Keywords:*
Chain mobility
Interfacial modification
Polarizability
Conductivity

ABSTRACT

The interfacial interactions and their effects on electrical properties are reported for thermally grown $SiO_2$–Parylene-C laminar composites. The segmental chain mobility of the interfacial Parylene-C was found to be enhanced in the composites. TSDC (thermally stimulated depolarization current) measurements showed the presence of dipolar interfacial energy states in these laminar composites. Functionalization of the oxide surface with 3-aminopropyltriethoxysilane (APTES) created dipolar energy states with larger activation energy at the interface between Parylene-C and $SiO_2$. In addition to the modification of interfacial states, incorporation of APTES interfacial layer also increased polarizability (real part of permittivity) and reduced the quasi-DC conductivity of laminar composites. The systematic changes in interfacial characteristics with thickness of APTES layer were explained based on structural orientation and cross linking of silane molecules.



## 1. Introduction

High energy density dielectrics reduce capacitor volume and weight in a wide array of applications including pulsed power systems and heart defibrillators with fast response. The capacitor energy density is related to the dielectric polarizability which is quantified by the permittivity of the dielectric ($K'$). High energy density capacitors must also have long-term stability, robust performance and high breakdown strength ($E_b$). Energy density ($U_e$) of a linear dielectric material is directly proportional to its permittivity ($K'$) and has a quadratic dependence over its breakdown strength ($E_b$). Hence nanocomposite materials made of high breakdown strength polymers as matrix and high dielectric constant oxides as fillers are an interesting system to study for high energy density capacitors [1]. Composite materials are particularly attractive because high energy density can be achieved with scalable manufacturing processes currently used to produce polymer films.

The energy stored ($U$) in composite dielectrics, which include 0–3, 2–2, and 1–3 systems with the numbers indicating connectivity of two constituent phases along three principal axes, is the summation of stored energy in constituent phases and in the interfacial volume between these phases [2,3]. However, individual phase contributions toward energy storage may also be augmented due to their interfacial modifications. The dispersion of nano-size ($<$100 nm) oxide particles in a polymer create a large interfacial volume, which is also shown to have a significant positive impact on the electrical properties of the composite dielectrics [4]. In order to store maximum energy, composite dielectrics must operate close to their breakdown limit and be dielectrically polarizable. Various breakdown mechanisms including electrical, thermal and electro-mechanical are discussed in detail by Dissado and Fothergill [5]. Intrinsic electrical strength and thermal breakdown strength both are controlled by various charge transport mechanisms, and ultimately the conductivity of the dielectric [5,6]. Charge transport often influence breakdown strength of a material and can be electronic as well as ionic. Presence of the deep energy states (traps) in a single phase dielectric material inhibits charge transport and hence may increase the breakdown strength [7]. In addition, energy states can be deliberately engineered in composite dielectrics at the interface of the oxide and the polymer phase [8]. The presence of high interfacial volume with the deep energy states at the interface in nanocomposites may potentially have a significant influence on charge transport and hence on energy density of the composite dielectrics.

Both the electrical and the mechanical properties of organic dielectrics are modified at interfaces. Presence of exponentially graded charge distribution at the interface, associated with the diffused double layer, can significantly influence the conductivity of the composite dielectrics as postulated by Lewis et al. [9,10]. Mechanical properties of interfacial polymers, such as modulus which is related to chain mobility are reported to be considerably different with respect to bulk polymers [11]. The coupling of interfacial electrical and mechanical properties in composite dielectrics, demonstrated by Ramesh et al., originates due to the overlap of

* Corresponding author. Fax: +1 814 865 2326.
*E-mail address:* put115@psu.edu (P. Tewari).

0021-9797/$ – see front matter 
doi:10.1016/j.jcis.2008.12.060

diffused double layer with the interfacial polymer with modified mechanical properties as suggested by Tanaka et al. [12,13]. The service life of the composite dielectric materials under high electrical stress can be significantly improved by enhancing the strength of interaction between the oxide and the polymer as demonstrated by Roy et al. [14]. The strength of interaction between the oxide and the polymer, which can be potentially engineered by a suitably chosen interfacial coupling agent, is shown to have significant impact on the interface permittivity as predicted using a saturation model proposed by Todd and Schi [15]. Incorporation of interfacial coupling agents was also found to significantly influence the conductivity of $BaTiO_3$–epoxy particulate composites [16].

A systematic electrical analysis of the interfacial effects in 0–3 and 1–3 particulate-based composite dielectrics is difficult due to the complicated mixture of series — parallel connectivity of interfaces, the percolation issues associated with the oxide particles and a complex local field distribution around particles of various sizes and shapes [17]. In the current work, laminar (2–2) thin film composites are proposed as a model system to understand the oxide–organic interfacial interactions and their effects on dielectric properties. Parylene-C is chosen as an organic layer due to its high reported breakdown strength (∼500 MV/m), low dielectric losses, and ease of deposition over a broad thickness range by vapor phase. Thermally grown silica (grown on high conductivity $p^{++}$ Si) is chosen as an inorganic phase due to its high insulating characteristics and minimal contribution from the Si–$SiO_2$ (electrode–oxide) interface. First, the electrical properties of the individual constituents and the laminar composite are fully characterized. Next, a qualitative analysis is carried out to study the effect of the interfacial layer of 3-aminopropyltriethoxysilane (APTES) on the electrical properties of the Parylene-C–silica laminar composite dielectrics. The current work highlights the importance of the interfacial effects in the oxide–organic composites and the role of interfacial modification to control polarizability and conductivity of composites.

## 2. Experimental work

### 2.1. Functionalization of silica surface

Thermally grown $SiO_2$ was functionalized with 3-aminopropyltriethoxysilane (APTES) using the dip coating technique. The silanization process was optimized on (100) single crystal Si (resistivity: 50–75 Ω cm) wafers. APTES was hydrolyzed by dissolving it in water. The solution was stirred for 24 hours. The pH of the solution was optimized in order to control the homocondensation of the organosilane (APTES) and hence promoting anchoring of APTES with the silica surface. In order to increase hydroxyl group density on the surface, Si and $SiO_2$ substrates were piranha cleaned. Piranha cleaned substrates were ultrasonicated in DI water and rinsed with ethanol before dipping in the APTES solution. The substrates were dipped for 45 min in the solution. After 45 min the solution was gently decanted and the wafers were baked at 115 °C overnight. Thicknesses of all the APTES films were characterized with the Gaertner L116C Variable Angle ellipsometer. The Bruker (IFS 66/5) spectrometer interfaced with the Bruker optical microscope was used to carryout the FT-IR analysis of the functionalized surface in transmission mode. Surface topography and surface roughness before and after functionalization were monitored using the tapping mode atomic force microscopy (carried out on Digital Instrument Nanoscope AFM).

### 2.2. Synthesis of Parylene-C films

The Parylene-C thin films were deposited on gold-sputtered alumina, thermally grown $SiO_2$ and APTES functionalized $SiO_2$ substrates using Parylene Labcoater system (PDS2010). During deposition the temperature of substrate was maintained at room temperature (RT). Synthesis was carried out under deposition conditions listed in Table 1. The process is discussed in detail by Sharma et al. [18]. As shown in Fig. 1, the rates of deposition of the Parylene-C thin films was controlled by adjusting the Parylene-C monomer pressure in the deposition chamber. The morphology of the Parylene-C thin films were studied by scanning electron micrographs (images were taken in back scattered electron mode on S3500N scanning electron microscope). The crystallite dimension of the Parylene-C thin films deposited at various conditions were analyzed using X-ray diffraction analysis (carried out using Cu $K_\alpha$ radiation) and Scherrer equation [19]. Peak broadening due to diffractometer was taken into account by obtaining a reference spectrum of the standard $LaB_6$ powder.

**Table 1**
Deposition parameters in Parylene-C synthesis.

| | |
|---|---|
| Evaporator temperature | RT to 160 °C |
| Pyrolysis temperature | 690 °C |
| Base pressure | 25 mtorr |
| Parylene-C monomer pressure | 9 mtorr to 28 mtorr |
| Substrate temperature | RT |

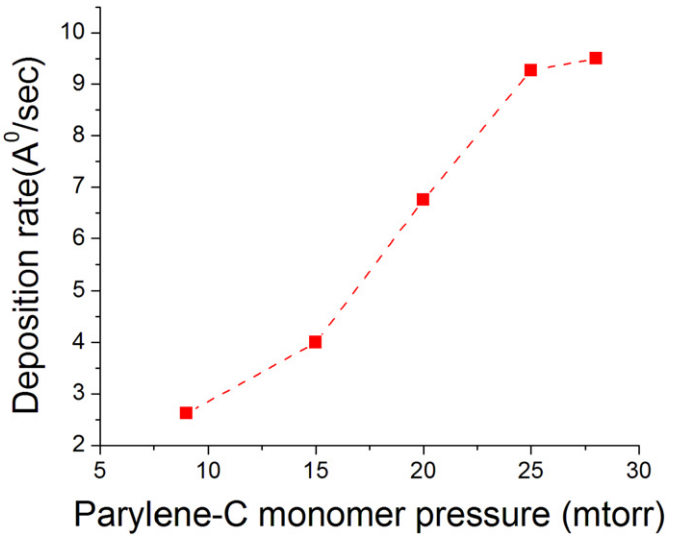


**Fig. 1.** Variation of deposition rate with pressure of Parylene-C monomer in deposition chamber (all analysis for 1 μm thick film).

### 2.3. Electrical characterization

Dielectric properties of individual phases (Parylene-C and thermally grown $SiO_2$) and of laminar composites were characterized using impedance spectroscopy and thermally stimulated depolarization current measurements. Impedance spectroscopy was carried out using dynamic signal analyzer (HP3562A) within the frequency range from 10 mHz to 1 kHz and with precision signal analyzer (HP4294A) from 1 kHz to 100 kHz. Real ($K'$) and imaginary ($K''$) part of permittivity were extracted from capacitance ($C$) and loss tangent ($\tan(\delta)$) measurements using the following equations:

$$K' = \frac{tC}{A\varepsilon_0}, \tag{1}$$

$$K'' = K' \tan(\delta). \tag{2}$$

Finally, the imaginary part of permittivity was converted to AC conductivity using the following relationship:

$$\sigma = \varepsilon_0 K'' \omega \tag{3}$$

where $t$, $A$, $\varepsilon_0$, $\omega$ and $\sigma$ are thickness of film, area of top electrode, permittivity of free space, angular frequency and AC conductivities respectively.

In thermally stimulated depolarization current (TSDC) measurements, samples were heated from room temperature to the poling temperature ($T_p$) under a poling electric field ($E_p$) for a fixed time ($t_p$). The samples were quenched with liquid nitrogen to a lower temperature ($T_0$) while maintaining poling field ($E_p$). After quenching the electric field was removed and sample temperature was raised with a constant heating rate ($q$). The depolarization currents were recorded with rising temperature. Recorded depolarization current spectrum was compared with Bucci–Fieschi theory for single relaxation, given by following equation:

$$J_D(T) = \frac{P_e(T_p)}{\tau_0} \exp\left(-\frac{E}{KT}\right) \exp\left[-\frac{1}{q\tau_0}\int_{T_0}^{T} \exp\left(-\frac{E}{KT'}\right) dT'\right] \quad (4)$$

where $K$, $q$, $P_e(T_p)$, $E$ and $\tau_0$ are Boltzmann constant, temperature ramp rate, polarization buildup at poling temperature, activation energy for relaxation and relaxation time constant at infinite temperature, respectively [20].

## 3. Results

### 3.1. Structural characterization

Crystallite dimension of Parylene-C for the $\alpha$-phase (having monoclinic crystal structure) was found to be 40–60 Å; more or less independent of deposition rate within the range of deposition rates shown in Fig. 1 [21]. However, scanning electron micrographs (as shown in Fig. 2) demonstrate that films deposited at low pressure and low deposition rate were more conformal, uniform and crack-free. The films deposited at high pressure and high deposition rate were rough and had nonuniform and poor dielectric properties. Hence, all the Parylene-C films were prepared at the minimum possible Parylene-C monomer pressure (~9 mtorr) in the deposition chamber. The crystallite dimension (as shown in Fig. 3) corresponding to the $\alpha$-phase (monoclinic crystal structure) in Parylene-C thin films was found to be linearly increasing with post-deposition annealing temperature up to 225 °C. Lee et al. have also reported a similar increase in crystallinity of Parylene-C film with high temperature post-deposition annealing [22]. In addition to enhancing film crystallite dimension, the electrical properties of the Parylene-C films were optimized by thermal annealing, and the annealed films (at 225 °C) were used as a baseline sample for all other laminar composite studies. Annealing the films at high temperature ensures that the polymer is in well-defined state during all electrical characterizations carried out in a wide temperature range.

FT-IR spectrum of the functionalized surface (shown in Fig. 4) clearly suggested the presence of amine functional group. All peaks seen in FT-IR spectrum are summarized in Table 2. As shown in Fig. 5, a control over thickness of APTES layer was achieved by controlling concentration of APTES solution during dip coating process. AFM images (shown in Fig. 6) of APTES functionalized (in the thickness ranges of 80 Å to 395 Å) (100) Si wafer showed a nonuniform growth of silane at lower thickness (~80 Å thickness) however films of higher thickness were found to be more uniform with roughness close to that of piranha cleaned Si wafer. Patchy nature of silane growth was also demonstrated by Eromosele et al. [23]. The roughness of functionalized surfaces (shown in Fig. 6) was calculated using tapping mode AFM. In order to eliminate effect of surface roughness in electrical analysis, electrical characterizations were carried out on composites with APTES layer in thickness range of 115 Å to 395 Å having comparable roughness.

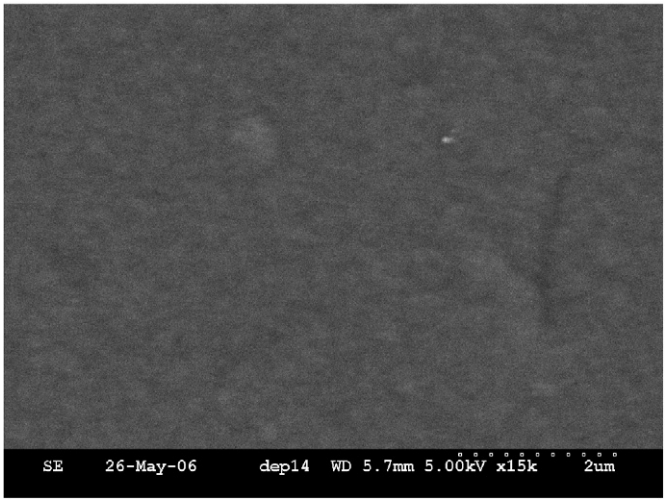


(a)

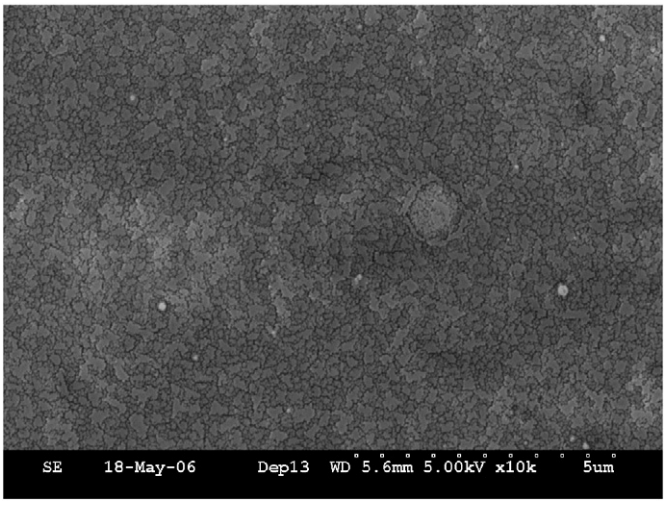


(b)

**Fig. 2.** SEM image of Parylene-C thin films deposited at (a) 9 mtorr and (b) 25 mtorr of Parylene-C monomer pressure.

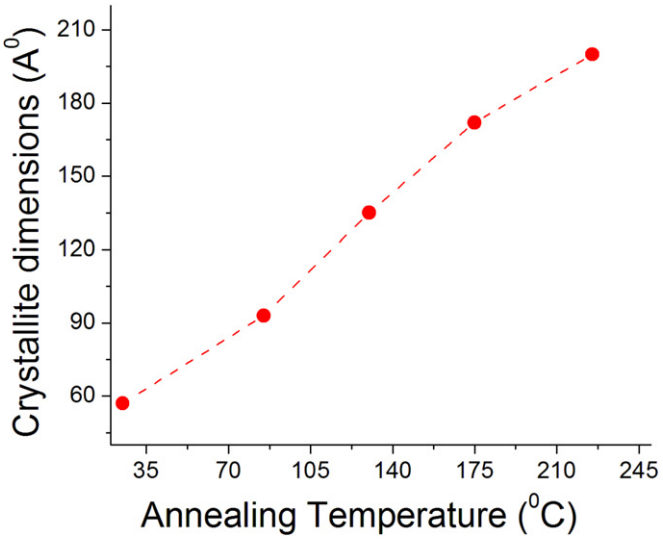


**Fig. 3.** Variation of crystallite dimension of $\alpha$-phase in Parylene-C thin films with post deposition annealing temperature (all analysis on 1 μm thick film, deposited on gold).

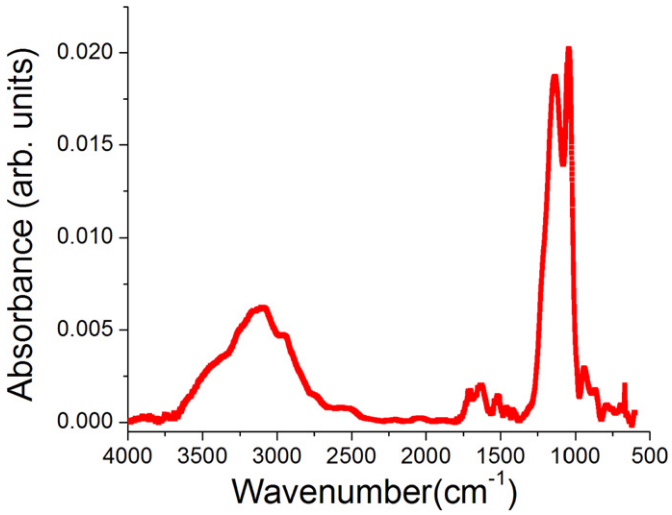


**Fig. 4.** FT-IR spectrum of APTES functionalized (100) Si wafer.

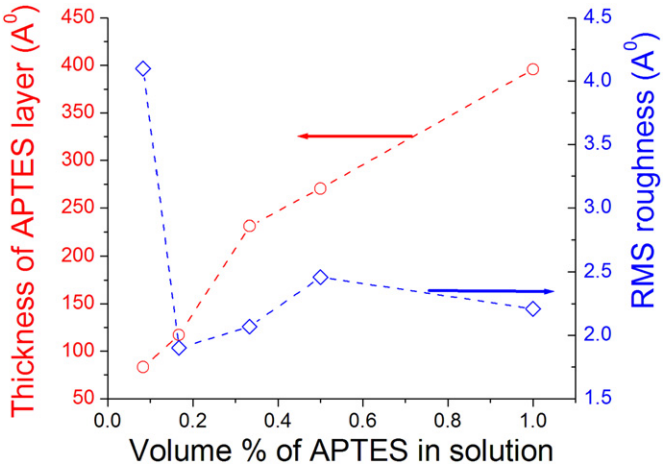


**Fig. 5.** Variation of APTES thickness on (100) Si wafer.

**Table 2**
Summary of FT-IR peaks of APTES functionalized (100) Si surface.

| Peak position ($cm^{-1}$) | Associated group | Vibration mode |
|---|---|---|
| 3110 | Primary amine | Stretching |
| 2960 | Alkane (–C–H) | Stretching |
| 1629 | Primary amine | Bending |
| 1136 and 1043 doublet | Siloxane (–Si–O–Si–) | Stretching |

### 3.2. Electrical properties

Impedance spectroscopy (as shown in Fig. 7) of Parylene-C thin films, deposited on gold, showed relaxation peaks in the temperature range of 98 °C to 192 °C. In Fig. 7b, the imaginary part of permittivity ($K''$) variation with frequency showed a strong shift of peak frequency ($F_{max}$) and small decrease of amplitude with increasing temperature, as shown previously for polyvinyl acetate [24]. Reduction in peak amplitude with increasing temperature without a change in shape of peak suggested a decrease in the total amount of relaxed dipoles with increasing temperature, which is an ideal characteristic of $\alpha$-relaxation associated with segmental motion [25,26]. The relaxation frequency is shown to follow the Arrhenius dependence over temperature. The Arrhenius dependence of the $\alpha$-relaxation frequencies with respect to temperature were previously reported for vinyl aromatic polymers and polyoxymethylene [27,28]. The activation energy for the $\alpha$-relaxation

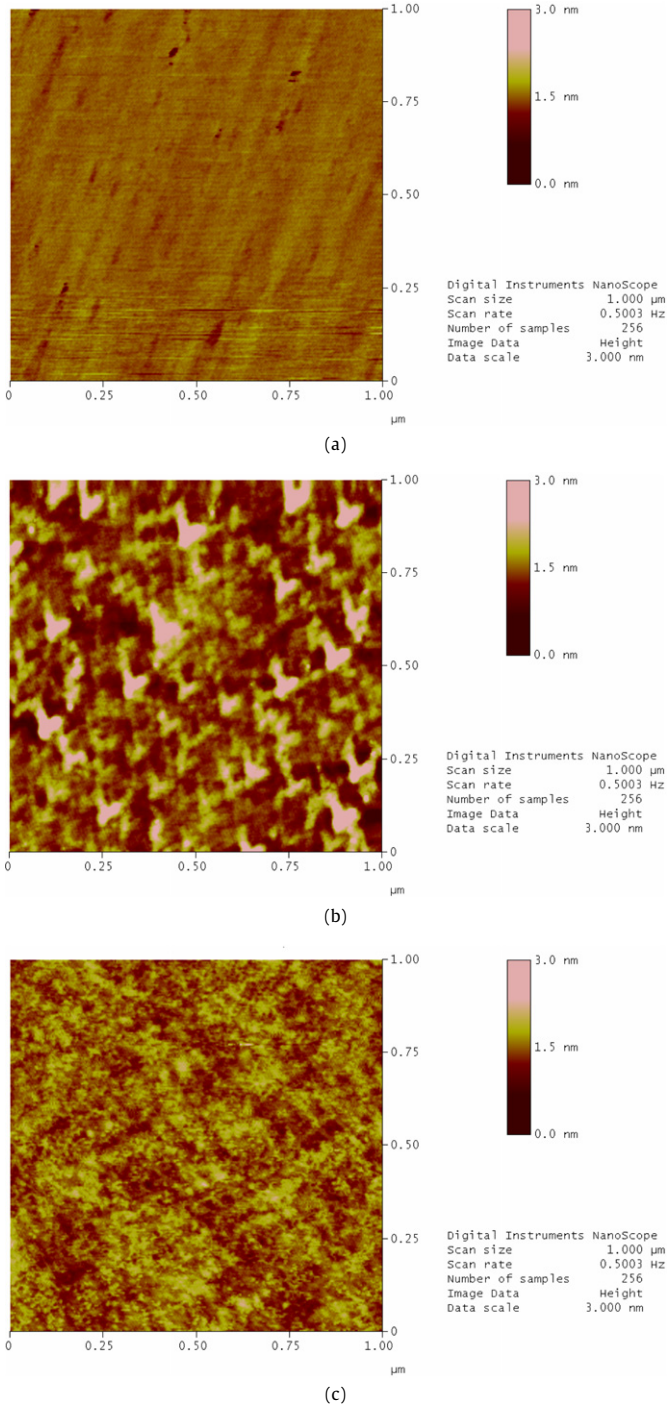


**Fig. 6.** Tapping mode AFM images of (a) (100) piranha cleaned Si wafer, (b) 83 Å thick APTES, (c) 395 Å thick APTES on (100) Si wafer.

in Parylene-C was found to be 1.37 eV. The complex capacitance plot of the Parylene-C films (Fig. 7c) is found to be asymmetric, suggesting a non-Debye type of relaxation. The thickness dependence dielectric studies of double layered $SiO_2$–Parylene-C dielectric suggested the presence of only one relaxation mechanism, corresponding to Parylene-C. However, the relaxation spectrum was found to be slightly shifted toward higher frequencies. As shown in Fig. 8, with a variation of Parylene-C thickness in the range of 500 nm to 7 µm, the activation energy and pre-exponential factor both show a monotonically increasing trend with their values approaching those of 1 µm Parylene-C thin films deposited on gold. Activation energy and pre-exponential factors (shown in Fig. 9),

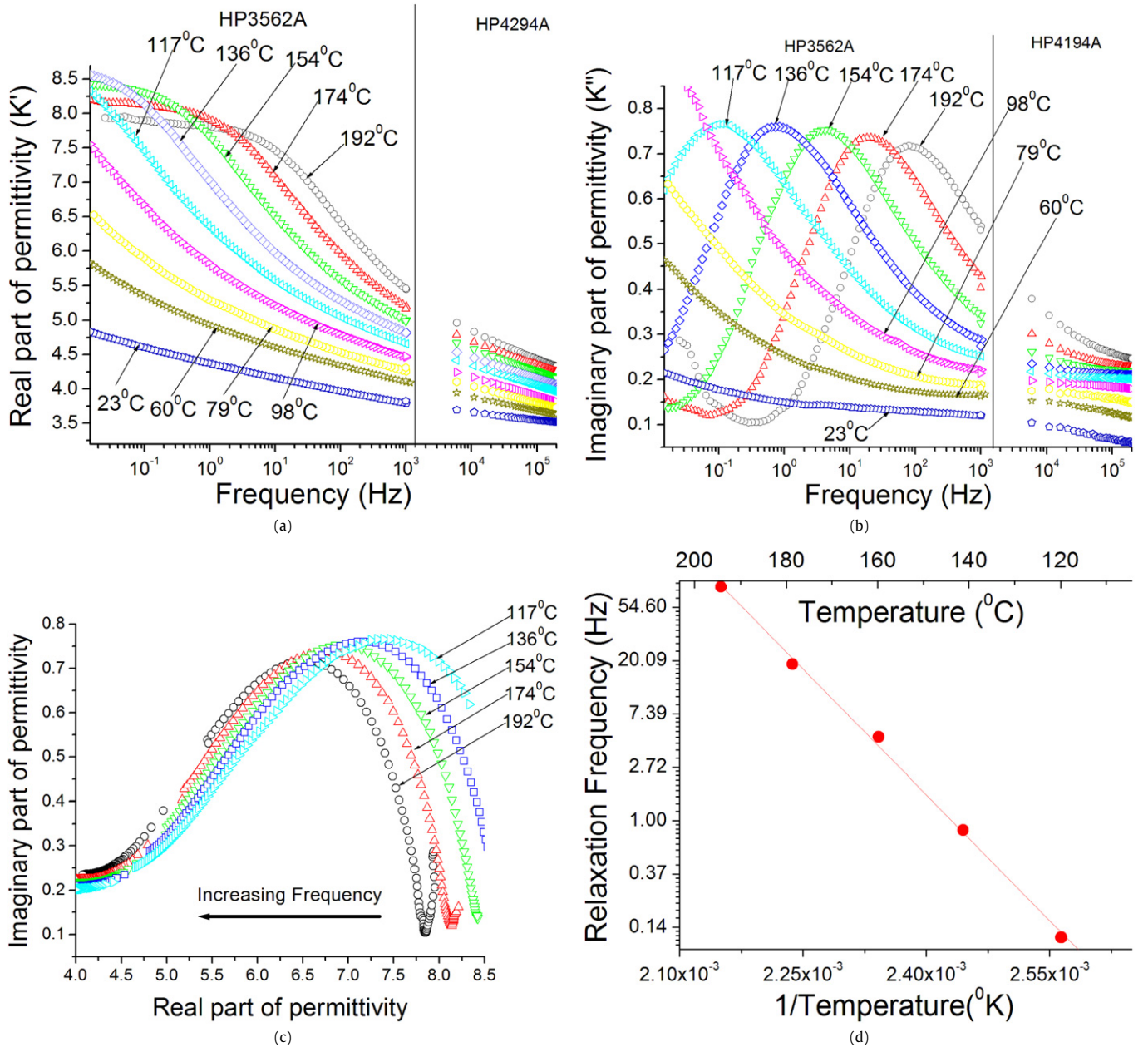


**Fig. 7.** Relaxation response of Parylene-C thin films. (a) Variation of real part of permittivity with frequency, (b) variation of imaginary part of permittivity with frequency, (c) complex capacitance plot, (d) Arrhenius dependence of relaxation frequency.

were also found to follow the Meyer–Neldel self-compensation law, reported to be related with cooperative dynamics of ionic motion and thermally activated jumps of low mobility charge carriers [29,30].

Thermally stimulated depolarization current (TSDC) measurements for Parylene-C were carried out by poling at an electric field of 40 MV/m for 20 min and by increasing temperature at 4 °C/min. As shown in Fig. 9a, TSDC spectrum of Parylene-C showed a peak at 70 °C which can be attributed to glass transition, observed in DSC analysis of Parylene-C. TSDC measurements on $SiO_2$ were carried out by poling at an electric field of 200 MV/m for 20 min and increasing temperature at 4, 8 and 12 °C/min. Lower poling field for Parylene-C thin films was chosen due to its degradation in insulating properties at high field and high poling temperature. The $SiO_2$ TSDC spectrum showed a peak close to 200 °C, which was previously reported to be due to presence of the trivalent Si atom associated with oxygen vacancies in $SiO_2$ [31]. In our analysis, the activation energy of this peak was found to be 0.20 eV. The thermally stimulated depolarization measurements of $SiO_2$–Parylene-C double layered dielectric structure carried out in field range of 75 MV/m to 300 MV/m (as shown in Fig. 10) showed glass transition peak as well as an additional peak in the temperature range of 150 to 165 °C. Apart from above mentioned peaks, a sharp peak was seen in the temperature range of 20 to 40 °C, which was attributed to the moisture [32]. The activation energy and time constant of additional peak were calculated using following expression:

$$T_m = \left[\frac{E}{K} q\tau_0 \exp\left(\frac{E}{KT_m}\right)\right]^{\frac{1}{2}} \tag{5}$$

where $T_m$, $E$, $K$, $q$ and $\tau_0$ are temperature maxima, activation energy, Boltzmann constant, temperature ramp rate and time con-

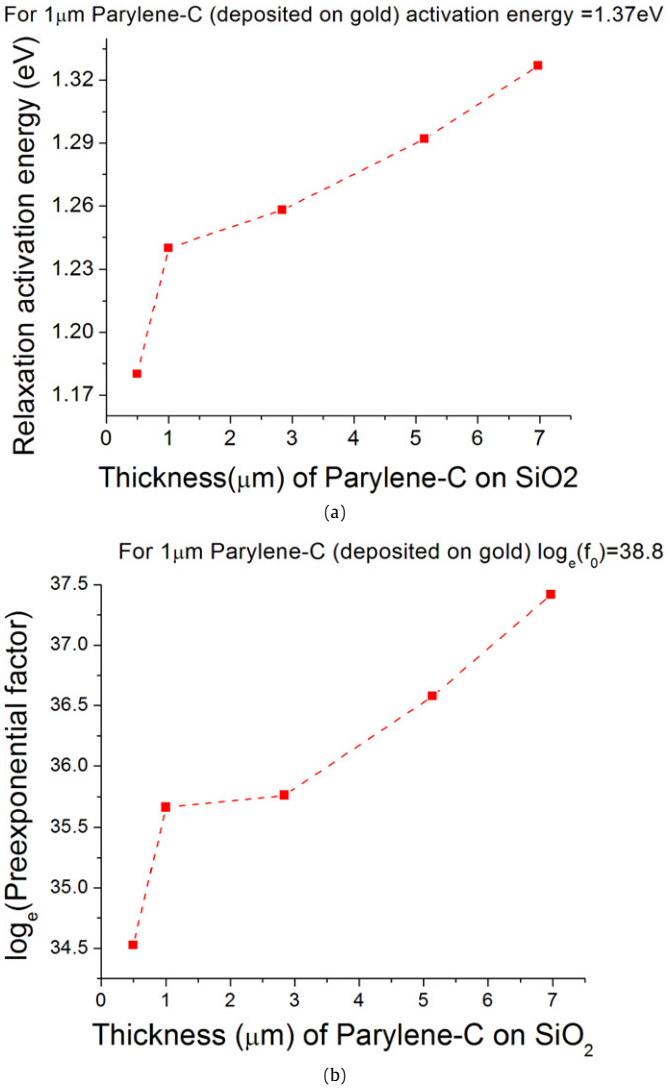


**Fig. 8.** Thickness dependence of (a) activation energy and (b) pre-exponential factor for relaxation in double layered composite dielectric.

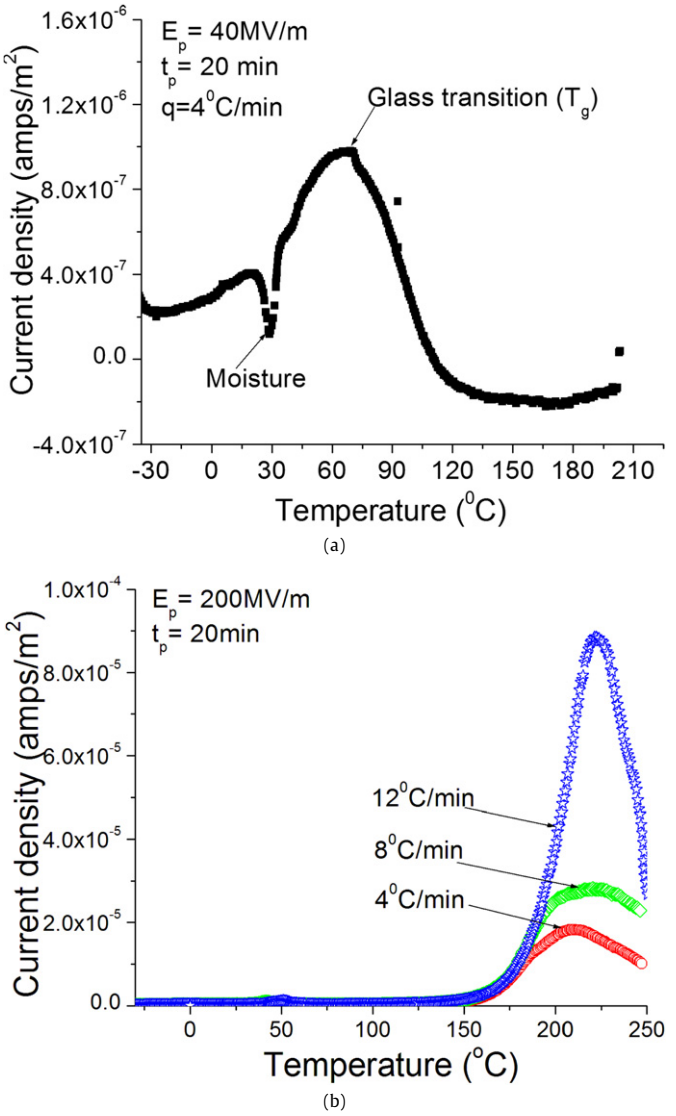


**Fig. 9.** Thermally stimulated depolarization current spectrum for (a) 1 μm thick Parylene-C and (b) 1 μm thick thermally grown $SiO_2$.

stant at infinite temperature associated with a interfacial TSDC peak [33].

Activation energy ($E$) and time constant at infinite temperature ($\tau_0$), evaluated using above expression and variation of additional peak maxima with different heating rates, were found to be distributed in a range shown in Fig. 11. The presence of this additional peak with different activation energy (1.05–1.30 eV) in the composite and its absence in the constituent phases suggested that the peak belongs to interfacial energy states. As shown in Fig. 10a, shift of interfacial peak toward higher temperature with increase in ramp rate was found to be consistent with the Bucci–Fieschi theory stated earlier. The fitting between activation energy and time constant at infinite temperature (shown in Fig. 11) was found to be qualitatively consistent with the Meyer–Neldel law [29]. The TSDC spectrum recorded with increasing poling field for the laminar composite (as shown in Fig. 10b) showed increase in interfacial peak height and its saturation close to 225 MV/m. A comparison of the TSDC spectra of the composites with and without APTES interfacial layer is shown in Fig. 12. A significant shift in the interfacial peak maxima toward higher temperature was observed with incorporation of APTES layer between $SiO_2$ and Parylene-C. As shown in Fig. 12, the temperature maxima of the interfacial peak shifted toward lower temperatures with an increase in thickness of APTES interfacial layer. The current density of the interfacial peak was found to be reduced with an increase in thickness of APTES layer between $SiO_2$ and Parylene-C. The glass transition peak was more or less unchanged with incorporation of APTES layer at the interface. As shown in Fig. 13, the real part of permittivity of the laminar composite with APTES interfacial layer was significantly higher (~25 to 30%) than for the composite without interfacial layer. Incorporation of APTES was also found to significantly reduce quasi-DC conductivity (shown in Fig. 14) of the composite. However, APTES interfacial layer had no appreciable influence on the conductivity of the composite at a higher frequency. The conductivity data is shown at 192 °C to identify clearly the regions of quasi-DC and AC conduction.

## 4. Discussion

Interfaces can play a critical role in determining the properties of nanocomposite dielectrics. High surface area of nanoparticles and small interparticle separation in nanocomposites (which is comparable to particle size) has been found to significantly influence the electrical properties of composite dielectrics [34,35]. Charge distributions at interface of oxide and polymer as well as presence of defect energy states may significantly influence the electrical properties of composite dielectrics. In this work, we re-

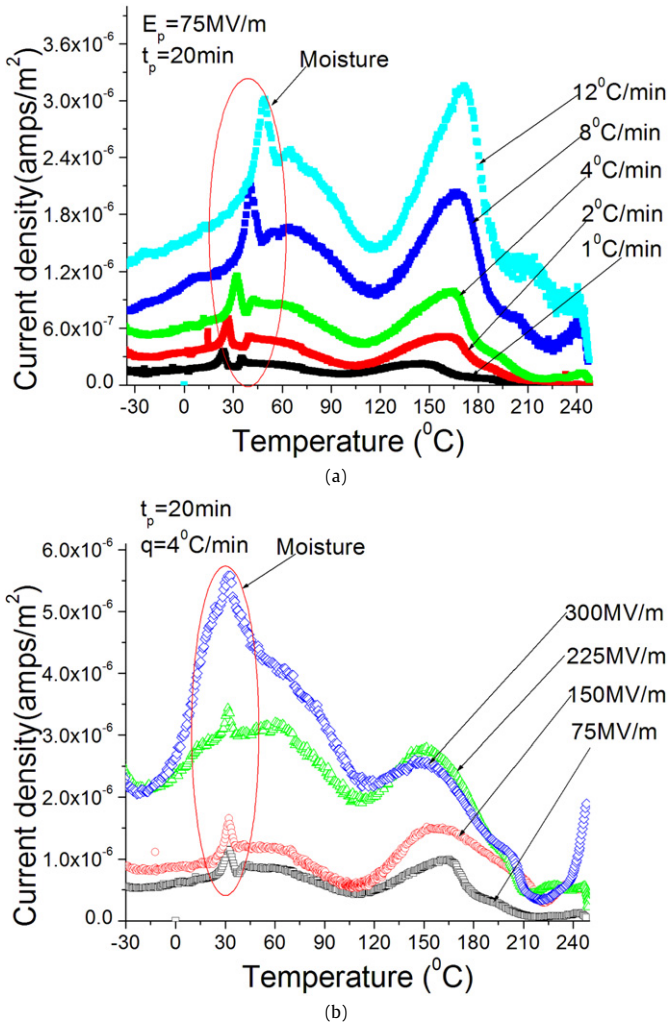


**Fig. 10.** Thermally stimulated depolarization current spectrum for laminar composite (1 μm $SiO_2$ + 1 μm Parylene-C). (a) Variation of heating rate at constant poling field of 75 MV/m, (b) variation of poling field at constant heating rate of 4 °C/min.

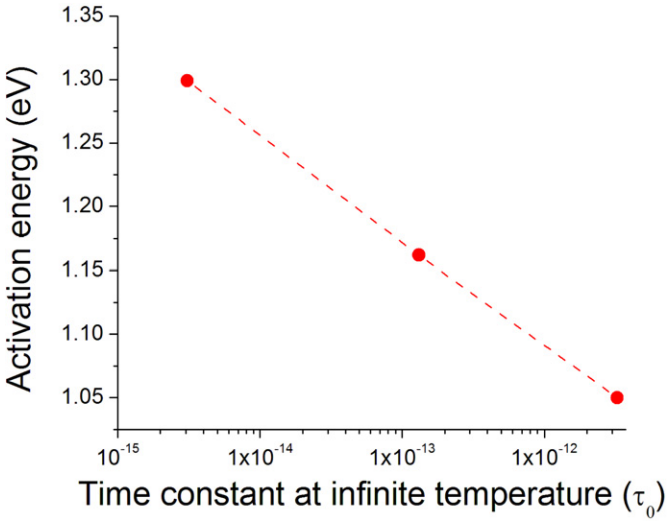


**Fig. 11.** Distribution of time constant ($\tau_0$) and activation energy for interfacial states.

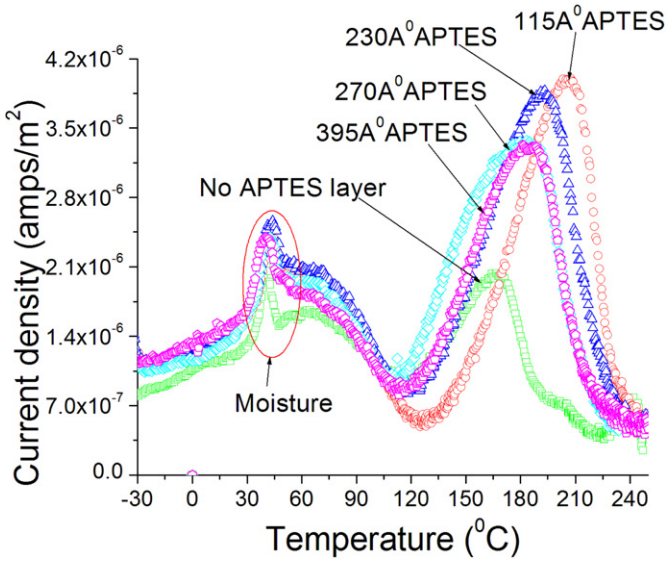


**Fig. 12.** Thermally stimulated depolarization current spectrum of laminar composite (1 μm $SiO_2$ + 1 μm Parylene-C) with and without APTES interfacial layer.

port the evidence of significant changes in segmental mobility of interfacial polymer, presence of defect energy states and their modification by functionalizing oxide surface with APTES coupling agent in $SiO_2$–Parylene-C laminar composite.

The impedance spectroscopy analysis of Parylene-C thin films showed relaxation related to segmental motion in the polymer. Lower values of $\alpha$-relaxation activation energy suggest higher segmental mobility of the polymer in laminar composite than of the polymer by itself (deposited on gold surface). This may be due to the difference in the interaction of Parylene-C with gold and $SiO_2$ surfaces as seen in PMMA films deposited on gold and native $SiO_2$ [36]. The reduction in the activation energy as well as the pre-exponential factor and their monotonically increasing values (as shown in Fig. 8) with thickness of Parylene-C, suggests enhanced segmental mobility only in the vicinity of $SiO_2$ and hence modification of the interfacial polymer. Our observation related to segmental mobility in the interfacial region may be due to several reasons such as differences in wetting characteristics of Parylene-C and $SiO_2$, modification in the crystallinity of the interfacial polymer; or change in glass transition temperatures of interfacial polymer in comparison to bulk polymers. The full width half maximum (FWHM) of the monoclinic phase ($\alpha$-phase) seen in XRD, was found to be unchanged (as shown in Table 3) in the thickness range of 75 nm to 6.72 μm, suggesting similar crystallite size in (in the range of 190–200 Å) for the interfacial and the bulk polymers. Possibility of changes in glass transition temperature with thickness (within given thickness range) was overruled, as variation of glass transition temperature is expected for polymer thickness comparable to radius of gyration [37,38]. The activation energy for $\alpha$-relaxation was found to be more or less unchanged with the incorporation of APTES layer suggesting no appreciable modification of polymer segmental mobility (on similar thickness scale) with surface fictionalization of $SiO_2$. Evidences of modification in segmental mobility were not evident in X-ray diffraction analysis (shown in Table 3), which may be due to non-subsurface nature of the technique. The unchanged peak position (in TSDC measurements) for glass transition with incorporation of APTES interfacial layer is also consistent with the unchanged mobility of the polymer chains.

Thermally stimulated depolarization current measurements of laminar composites showed the presence of interfacial energy states. Saturation of the depolarization current peak (corresponding to interfacial states) with the poling field suggested the dipolar nature of the interfacial states. Formation of a dipole at interface of $SiO_2$ and Parylene-C is likely due to wide differences in the polarity of two surfaces, as evident from hydrophilic nature of $SiO_2$ surface

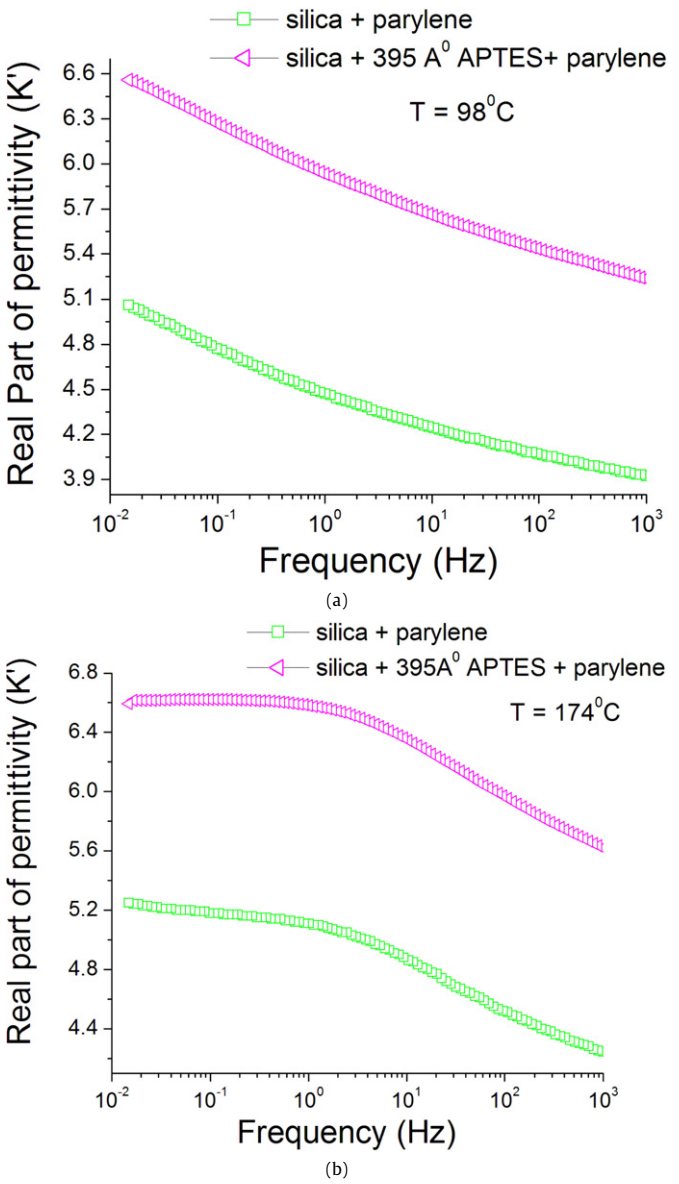


**Fig. 13.** Comparison of real part of permittivity for laminar composite with and without APTES interfacial layer (a) at 98 °C and (b) 174 °C.

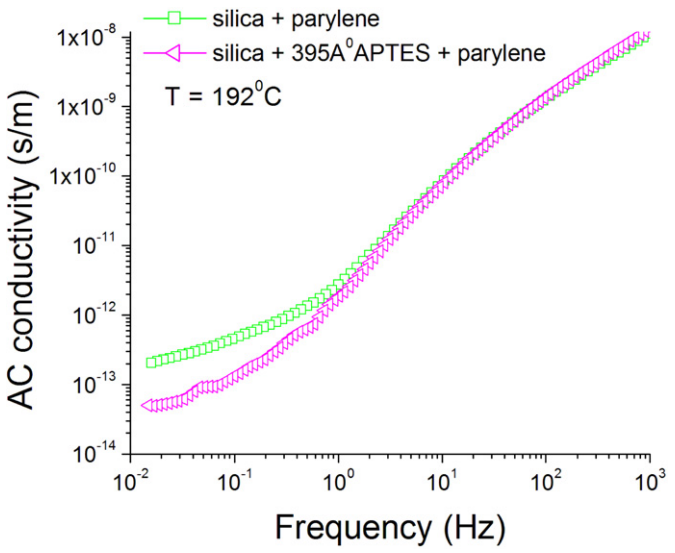


**Fig. 14.** Comparison of conductivity of laminar composites with and without APTES.

**Table 3**
X-ray diffraction FWHM analysis of monoclinic phase in Parylene-C film.

| Sample name | FWHM (°) of monoclinic ($\alpha$) phase peak seen in X-ray diffraction |
|---|---|
| $SiO_2$ + 75 nm Parylene-C | 0.617 (0.051) |
| $SiO_2$ + 660 nm Parylene-C | 0.586 (0.008) |
| $SiO_2$ + 1.2 μm Parylene-C | 0.571 (0.005) |
| $SiO_2$ + 3.17 μm Parylene-C | 0.577 (0.005) |
| $SiO_2$ + 6.72 μm Parylene-C | 0.581 (0.005) |
| 1 μm Parylene-C on gold sputtered $Al_2O_3$ | 0.568 (0.008) |
| $SiO_2$ + APTES + 1.2 μm Parylene-C | 0.600 (0.083) |

and hydrophobic nature of Parylene-C surface [39,40]. Incorporation of APTES interfacial layer was found to generate deeper energy states at the interface, which was shown as a shift in interfacial peak maxima toward higher temperatures. A significant increase in the depolarization current density for the interfacial states by incorporating APTES interfacial layer suggested that the addition of amine functional silane at the interface of $SiO_2$ and Parylene-C can significantly enhance the polarizability of laminar composite. Due to small volume fraction of APTES (0.4–1.5%) in these laminar structures, such a large increase in polarizability cannot be explained by series mixing rules. Additional leakage contributions toward depolarization current were ruled out as surface modification of $SiO_2$ with APTES was found to reduce quasi-DC conductivity of laminar composite. The increase in dielectric permittivity (~25 to 30%) of the composite with incorporation of APTES interfacial layer also confirmed increase in the polarizability of the composite.

The increased polarizability of the lamellar composite may be either due to the modification in the growth of Parylene-C thin film on APTES functionalized $SiO_2$ or modification in interaction between $SiO_2$ and Parylene-C due to incorporation of APTES interfacial layer or due to addition of dipoles at interface with functionalization of the $SiO_2$ surface. Amine functional silane has been previously shown to enhance the interaction between $BaTiO_3$ and PVDF and hence increase the polarizability of the particulate (0–3) composites [41]. However, modifications in the interaction between $SiO_2$ and Parylene-C was not evident in the FT-IR spectrum (not shown here) of functionalized and unfunctionalized composites, which may be due to small interfacial area in laminar composites in comparison to particulate–polymer composites. The reduction in depolarization current density with an increase in thickness of APTES interfacial layer suggested a reduction in the polarizability of the composite. Reduction in the polarizability of composite with an increase in the thickness of APTES layer may be due to a reduced structural orientation of the thick APTES films in comparison to thinner layers. The reduced orientation in multilayer compared to monolayer silanes was previously demonstrated by Hied and Effenberger for trichlorosilanes [42]. Shift in the interfacial peak maxima toward lower temperature with an increase in the thickness of APTES interfacial layer suggested reduction in activation energy for dipolar relaxation. Reduction in activation energy, signifying ease of dipolar relaxation, may be due the presence of partially cross linked silane molecules in thick APTES layer in comparison to thinner APTES layer. The experiments conducted in this study suggested that enhanced dielectric polarizability and reduced quasi-DC conductivity, the two main parameters in high energy density materials, can be achieved by suitably modifying interfaces in composite dielectrics.

## 5. Conclusions

Silica–Parylene-C laminar composites were synthesized and characterized to study the role of interfaces and their modifi-

cations on dielectric properties of laminar composite dielectrics. Interfacial modification of laminar composite was carried out by functionalizing thermally grown $SiO_2$ with APTES coupling agent. The thickness control over APTES layer was achieved by controlling the volume fraction of APTES in a solution during the dip coating process. The activation energy for segmental motion of Parylene-C in the laminar composite was found to be lower than for Parylene-C itself, suggesting an enhancement in the segmental mobility of Parylene-C in the laminar composite. Thickness dependence studies showed enhancement in the chain mobility of Parylene-C only in the interfacial region of the laminar composite. Thermally stimulated depolarization current measurements showed the presence of dipolar energy states at the interface with activation energy in the range of 1.05 to 1.30 eV. Interfacial modification with APTES coupling agent was found to generate deeper dipolar states at the interface, reduce quasi-DC conductivity and increase polarizability of the composite which was shown as an increase in the depolarization current density and increase in the dielectric permittivity. A systematic shift in interfacial peak maxima toward lower temperature and reduction in the depolarization current density with an increase in the thickness of APTES interfacial layer may be due to the presence of partially cross linked silane molecules and reduced structural orientation in thicker APTES films.

## Acknowledgments

The authors would like to thank Jeff Long and Paul Moses for help in electrical characterization. The authors would also like to thank Dr. Nadine Smith and Gene Gerber for the use of their Parylene deposition system. The Office of Naval Research sponsored this work under grant N00014-05-1-0541.

## References

[1] Y. Cao, P.C. Irwin, K. Younsi, IEEE Trans. Diel. Electr. Insul. 11 (2004) 797.
[2] J.F. Tressler, S. Alkoy, A. Dogan, R.E. Newnham, Compos. Part A Appl. Sci. Manufact. 30 (1999) 477.
[3] B. Chu, M. Lin, B. Neese, X. Zhou, Q. Chen, Q.M. Zhang, Appl. Phys. Lett. 91 (2007) 122909.
[4] J.K. Nelson, L.A. Utracki, R.K. MacCrone, C.W. Reed, Annual Report-CEIDP, 2004, p. 314.
[5] L.A. Dissado, J.C. Fothergill, Electrical Degradation and Breakdown in Polymers, Peter Peregrins Ltd., London, 1992.
[6] J.J. O'Dwyer, The Theory of Electrical Conduction and Breakdown in Solid Dielectrics, Clarendon Press, Oxford, 1973.
[7] T. Tanaka, IEEE Trans. Diel. Electr. Insul. 12 (2005) 914.
[8] N. Schi, R. Ramprasad, IEEE Trans. Diel. Electr. Insul. 15 (2008) 170.
[9] T.J. Lewis, J. Phys. D Appl. Phys. 38 (2005) 202.
[10] T.J. Lewis, IEEE Trans. Diel. Electr. Insul. 11 (2004) 739.
[11] E. Ho, M. Marcolongo, Dental Mater. 21 (2005) 656.
[12] S. Ramesh, B.A. Shutzberg, C. Huang, J. Gao, E.P. Giannelis, IEEE Trans. Adv. Pack. 26 (2003) 17.
[13] T. Tanaka, M. Kozako, N. Fuse, Y. Ohiki, IEEE Trans. Diel. Electr. Insul. 12 (2005) 669.
[14] M. Roy, J.K. Nelson, R.K. McCrone, L.S. Schadler, C.W. Reed, R. Keefe, W. Zeneger, IEEE Trans. Diel. Electr. Insul. 12 (2005) 629.
[15] M.G. Todd, F.G. Schi, J. Appl. Phys. 94 (2003) 4551.
[16] L. Ramajo, M.S. Castro, M.M. Reboredo, Compos. Part A 38 (2007) 1852.
[17] Y. Nakajima, T. Matsuyama, J. Electrostat. 55 (2002) 203.
[18] A.K. Sharma, A.W. Hahn, M.F. Nichols, J. Appl. Polym. Sci. 36 (1988) 1555.
[19] V. Uvarov, I. Popov, Mater. Charact. 58 (2007) 883.
[20] V.M. Gun'ko, V.I. Zarko, E.V. Goncharuk, L.S. Andriyko, V.V. Turov, Y.M. Nychipourk, R. Leboda, J. Skubiszewska-Zeiba, A.L. Gabchak, V.D. Osovikii, Y.G. Ptushinskii, G.R. Yurchenko, O.A. Mishchuk, P.P. Pissis, J.P. Blitz, Adv. Colloid Interface Sci. 131 (2007) 1.
[21] H.L. Huang, Y. Xu, H.Y. Low, Polymer 146 (2005) 5949.
[22] J.H. Lee, K.S. Hwang, K.H. Yoon, T.S. Kim, S. Ahn, IEEE Trans. Plasma Sci. 32 (2004) 505.
[23] I.C. Eromosele, D.C. Pepper, B. Ryan, Macromol. Chem. Phys. 190 (1989) 1613.
[24] A.K. Jonscher, Dielectric Relaxation in Solids, Chelsea Dielectrics Press, London, 1983.
[25] G.G. Raju, Dielectrics in Electric Field, Marcel Dekker, New York, 2003.
[26] V.A. Bershtein, V.M. Yegorov, Yu.A. Yemel'yanov, Polym. Sci. USSR 27 (1985) 2757.
[27] J.M. Pochan, D.F. Hinman, J. Polym. Sci. 14 (1976) 2285.
[28] S. Shimada, Y. Hori, H. Kashiwabra, Polymer 22 (1981) 1377.
[29] K.L. Ngai, Solid State Ionics 105 (1998) 231.
[30] I.M. Daveltabayeva, V.V. Parfenov, V.P. Dorozhkin, P.A. Kirpichnikov, Polym. Sci. USSR 31 (1989) 1331.
[31] D.M. Fleetwood, P.S. Pinokur, L.C. Reiwe, R.A. Reber Jr., J. Appl. Phys. 84 (1998) 6141.
[32] E. Rysiakeiwicz, J. Electrostat. 51–52 (2001) 173.
[33] P. Bräunlish, Thermally Stimulated Relaxation in Solids, Springer-Verlag, Berlin, 1979.
[34] T. Imai, F. Sawa, T. Nakano, T. Ozaki, T. Shimizu, M. Kozako, T. Tanaka, IEEE Trans. Diel. Electr. Insul. 13 (2006) 319.
[35] M. Roy, J.K. Nelson, R.K. McCrone, L.S. Schadler, J. Mater. Sci. 42 (2007) 3789.
[36] J.L. Keddie, R.A.L. Jones, R.A. Corey, Faraday Discuss. 98 (1994) 219.
[37] C.B. Roth, J.R. Dutcher, J. Electroanal. Chem. 584 (2005) 13.
[38] Y. Pu, M.H. Rafailovivh, J.H. Sokolov, D. Gersappe, T. Peterson, W.-L. Wu, S. Schwarz, Phys. Rev. Lett. 87 (2001) 206101.
[39] D. Janssen, R.D. Palma, S. Verlaak, P. Heremans, W. Dehaen, Thin Solid Films 515 (2006) 1433.
[40] J.T. Yang, J.C. Chen, J.J. Chuang, J.A. Yeh, J. Microelectromech. Syst. 15 (2006) 697.
[41] Z.M. Dang, H.Y. Wang, H.P. Xu, Appl. Phys. Lett. 89 (2006) 112902.
[42] S. Heid, F. Effenberger, Langmuir 12 (1996) 2118.